

Journal of Materials Chemistry B

Accepted Manuscript



This is an *Accepted Manuscript*, which has been through the RSC Publishing peer review process and has been accepted for publication.

Accepted Manuscripts are published online shortly after acceptance, which is prior to technical editing, formatting and proof reading. This free service from RSC Publishing allows authors to make their results available to the community, in citable form, before publication of the edited article. This *Accepted Manuscript* will be replaced by the edited and formatted *Advance Article* as soon as this is available.

To cite this manuscript please use its permanent Digital Object Identifier (DOI®), which is identical for all formats of publication.

More information about *Accepted Manuscripts* can be found in the [Information for Authors](#).

Please note that technical editing may introduce minor changes to the text and/or graphics contained in the manuscript submitted by the author(s) which may alter content, and that the standard [Terms & Conditions](#) and the [ethical guidelines](#) that apply to the journal are still applicable. In no event shall the RSC be held responsible for any errors or omissions in these *Accepted Manuscript* manuscripts or any consequences arising from the use of any information contained in them.

Cite this: DOI: 10.1039/c0xx00000x

ARTICLE TYPE

www.rsc.org/xxxxxx

Silver nanoparticles/ionic silsesquioxane: a new system proposed as antibacterial agent

Andressa C. Schneid,^a Eliane W. Roesch,^b Fernanda Sperb,^b Ursula Matte,^b Nádyá P. da Silveira,^a Tania M. H. Costa,^a Edilson V. Benvenutti,^{*a} and Eliana W. de Menezes^{*a}

5

Received (in XXX, XXX) Xth XXXXXXXXXX 20XX, Accepted Xth XXXXXXXXXX 20XX

DOI: 10.1039/b000000x

Spherical silver nanoparticles with average size *ca.* 5 nm were synthesized in aqueous medium using as stabilizer and size controller a charged silsesquioxane containing quaternary ammonium group, the bridged 1,4-diazoniabicyclo[2.2.2]octane nitrate. For the first time this system was synthesized and applied as antibacterial agent and its activity was confirmed with excellent results. The new system shows high stability, which can be confirmed by unchanged UV-Vis band even one year later. The magnitude of zeta-potential (ζ) (+24.7 mV) indicated electrostatic contribution for the silver nanoparticles stability and the signal showed that the nanoparticles have a positively charged surface. *In vitro* antibacterial tests were performed against *E. coli*, *P. aeruginosa* and *S. aureus* bacteria, and the minimum concentration of silver in the nanoparticles form for complete inhibition of bacteria were 0.60, 1.1 and 2.0 $\mu\text{g mL}^{-1}$, respectively. These values are very low if compared to the previous reports, making this system very promising. Cytotoxicity assay showed that these silver nanoparticles are safe for mammalian cells at the studied concentrations.

Introduction

Metal nanoparticles exhibit unique physical, chemical, electrical and optical properties that may differ significantly from metallic ion and bulk metals.¹⁻³ These properties are mainly determined by size, shape, composition, crystallinity and structure of the nanoparticles, enabling broad applications in several fields as catalysts, electronic, magnetic, optical and environmental devices.²⁻⁹

The synthesis route of metal nanoparticles has a major influence on their size, shape and optical properties. Generally, metal nanoparticles can be prepared by both physical and chemical methods. However, the chemical approach, such as reduction of metallic cations, is the most widely used. The synthesis of nanoparticles by different reduction methods is often performed in the presence of stabilizers in order to prevent unwanted agglomeration. The addition of stabilizers such as polymers, dendrimers, biopolymers, micelles, microemulsions, ionic liquids, surfactants or thiols, has resulted in an efficient way to avoid the agglomeration process of nanoparticles.^{2,8-12}

Among the metal nanoparticles, the silver ones have been widely applied in medical field due to their effective activity against a broad spectrum of microorganisms including bacteria, yeast and fungi, even at very low concentration.^{5,11-17} The antibacterial activity of silver nanoparticles containing materials can be used to treat burns and a variety of infections. Silver nanoparticles have a high specific surface area and a high fraction of surface atoms that lead to high antimicrobial activity compared

to bulk silver metal. It has been proposed that silver nanoparticles may adhere to the cell wall, thus disturbing cell-wall permeability and cellular respiration.^{18,19} The nanoparticles may also penetrate inside the cell causing damage by interaction with phosphorus- and sulfur-containing compounds such as DNA and protein.^{20,21} Other possible mechanism to the activity of the silver nanoparticles is the release of silver ions from particles, which will have an additional contribution to the bactericidal properties.²¹ It has been also suggested that the antimicrobial mechanism of silver nanoparticles may also be related to the membrane damage caused by free radicals that are derived from the surface of the nanoparticles.¹⁹ Additionally, the bactericidal activity also appears to be dependent on the size and shape of the silver nanoparticles.¹⁸

Recently, it has been reported that charged or ionic silsesquioxanes, which are hybrid materials synthesized from gelation of organosilanes that contain quaternary ammonium groups, may be applied as stabilizers and size controllers of gold nanoparticles with diameters lower than 15 nm, in aqueous medium.^{22,23} In this case, the synthesis of metal nanoparticles was based on reduction of metal salts in solution containing ionic silsesquioxane. The solubility of these charged hybrid materials in polar solvents,^{24,25} due to the presence of the quaternary ammonium groups, accounts for the stability of aqueous dispersion of nanoparticles. Additionally, the quaternary ammonium groups are also known for their inhibitory and antimicrobial effects,²⁶⁻³³ considering that their antibacterial use is prior to the silver nanoparticles one.²⁶ Thus this aqueous silver nanoparticles/silsesquioxane system is a particularly important

proposal because, besides being compatible to the environment in biological systems, it combines the antibacterial activity of both, silver nanoparticles and quaternary ammonium compounds.

In this work, silver nanoparticles were synthesized in aqueous medium using an ionic silsesquioxane containing the quaternary ammonium group, the bridged 1,4-diazoniabicyclo[2.2.2]octane nitrate. The ionic silsesquioxane was characterized by X-ray diffraction, ^{13}C -NMR, ^{29}Si -NMR and the silver nanoparticles dispersion was characterized by UV-Vis, TEM and zeta (ζ)-potential. The antibacterial activity of the silver nanoparticles/silsesquioxane was evaluated for three types of bacteria: *Staphylococcus aureus*, *Escherichia coli* and *Pseudomonas aeruginosa* and the cytotoxicity was evaluated using the Baby Hamster Kidney (BHK) cell line through the MTT assay.

Experimental

Chemicals

3-chloropropyltrimethoxysilane (CPTMS), 1,4-diazabicyclo[2.2.2]octane (DABCO) and N,N-dimethylformamide were purchased from Aldrich. Methanol and hydrofluoric acid were obtained from Merck. Formamide, silver nitrate and sodium borohydride were acquired from Vetec and sodium nitrate was purchased from Neon. Broth for bacteria growth was purchased from Merck. Cell culture medium (DMEM) and supplements (fetal calf serum and penicillin/streptomycin) were purchased from Invitrogen (USA). All chemicals employed were of analytical grade and used as received without any further purification.

Synthesis of ionic silsesquioxane

The ionic silsesquioxane containing the 1,4-diazoniabicyclo[2.2.2]octane nitrate group, was synthesized as follows. In the first step of the synthesis, 5.605 g of DABCO were dissolved in 40 mL of N,N-dimethylformamide, under argon atmosphere. After that, 11.4 mL of CPTMS were added. The mixture was heated at 80 °C, upon stirring for 72 h, under inert atmosphere, until a white solid was formed. This solid was washed with methanol and dried for 2 h at 70 °C to obtain a purified ionic organosilane precursor, represented in Figure 1A. In sequence, the organosilane precursor was dissolved in 40 mL of formamide, under constant stirring at 70 °C, and 0.8 mL of water containing five drops of hydrofluoric acid was added. The mixture was stored for gelation and evaporation of solvent at 40 °C to obtain the silsesquioxane that contain the bridged 1,4-diazoniabicyclo[2.2.2]octane chloride group, hereafter designated as $\text{SiDb}(\text{Cl})_2$ (Figure 1B). The last step consists in an ion exchange process where the chloride was replaced by nitrate using cold NaNO_3 1 mol L^{-1} solution, which was evaluated by chloride potentiometric analysis with AgNO_3 solution. Afterwards, the solid was heated at 50 °C under vacuum to eliminate the residual solvent. The resulting water soluble silsesquioxane material, which contains the 1,4-diazoniabicyclo[2.2.2]octane nitrate group, hereafter designated by $\text{SiDb}(\text{NO}_3)_2$ (Figure 1C), was used for synthesis of silver nanoparticles.

Synthesis of silver nanoparticles

Aqueous solution (10.0 mL) containing 100 mg of ionic

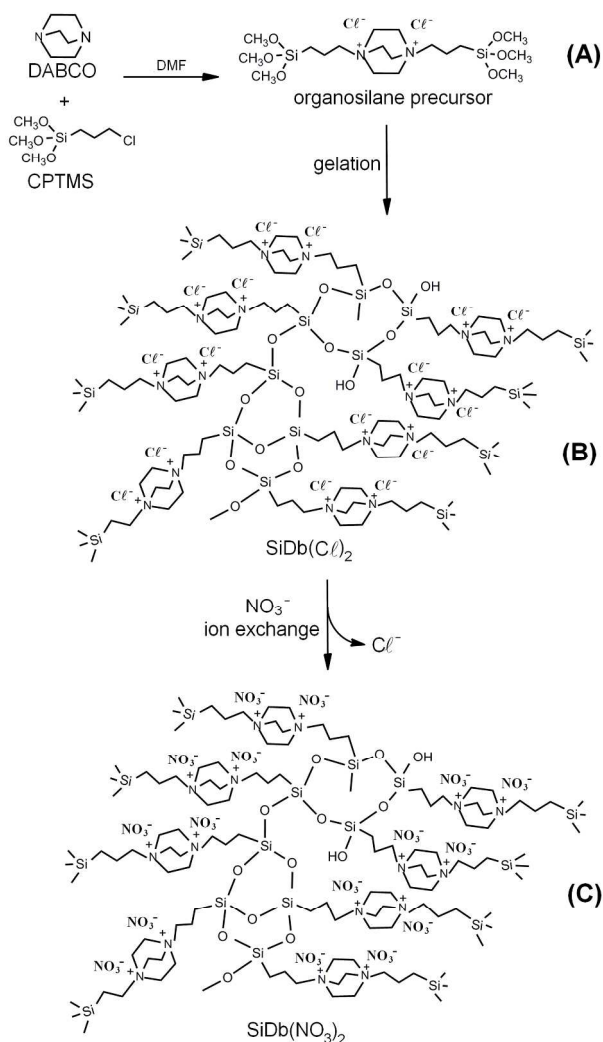


Fig 1. Schematic representation of the $\text{SiDb}(\text{NO}_3)_2$ synthesis.

silsesquioxane $\text{SiDb}(\text{NO}_3)_2$ was mixed with 1.0 mL of 1.5×10^{-3} mol L^{-1} AgNO_3 . Shortly after that, 5 mL of 0.02 mol L^{-1} NaBH_4 freshly prepared were added to the mixture, always under stirring. The aqueous colloidal dispersion of silver nanoparticles, stabilized by ionic silsesquioxane was designated by AgNPs. In these conditions the concentration of divalent 1,4-diazoniabicyclo[2.2.2]octane nitrate group was 11.3×10^{-6} mol mL^{-1} , and the concentration of silver atoms was 93.8×10^{-9} mol mL^{-1} , in the form of nanoparticles, corresponding to 10.1×10^{-6} g mL^{-1} of silver. For comparison with AgNPs dispersion, a reference solution, without metal addition, was also prepared, and it was designated as blank.

Characterization

X-ray diffraction (XRD) measurement of the powdered ionic silsesquioxane was carried out by Siemens diffractometer model D500 using $\text{CuK}\alpha$ as X-ray source ($\lambda = 0.154056$ nm) at a generator voltage of 40 kV and a generator current of 17.5 mA. CP MAS ^{13}C and ^{29}Si NMR spectra were performed on a varian500-nmrs spectrometer. The measurements were made utilizing pulse length of 16 ms and recycle delay of 5 s. The UV-Visible spectra of AgNPs were carried out in the range between 300 and 600 nm, at room temperature, using a UV-160 1P

Shimadzu spectrophotometer, and distilled water was used as reference. Transmission Electron Microscopy (TEM) images of AgNPs aqueous dispersion were recorded using a JEOL JEM-1220 microscope, operated at an acceleration voltage of 120 kV. Samples for TEM images were prepared by placing two drops of the aqueous AgNPs dispersion onto a carbon-coated Cu grid, followed by drying at ambient conditions. The size distribution of the silver nanoparticles was determined using the Quantikov software. X-ray photoelectron spectra (XPS) were also obtained for evaporated sample using a hemispheric Specs VSW HA 100 spectrometer, with 20 h of acquisition time. The zeta (ζ)-potential was determined in water at room temperature using a ZetaPALS Potential Analyzer (Brookhaven Instruments Corp.). The ZetaPALS utilizes analysis phase light scattering to measure the electrophoretic mobility of charged colloid. The software then converts these electrophoretic mobility data into ζ -potential values based on the Smoluchowsky's equation.

20 Antibacterial activity tests

Antibacterial activity of the ionic silsesquioxane/AgNPs system was tested against three species of bacteria. One species, *Staphylococcus aureus* (*S. aureus*, ATCC 25923) is representative for Gram-positive bacteria, while *Escherichia coli* (*E. coli*, ATCC 25922) and *Pseudomonas aeruginosa* (*P. aeruginosa*, ATCC 27853) are Gram-negative. The cultures were grown in Tryptic Soy Broth (TSB, Merck) at a concentration of 1×10^8 Colony Forming Units per mL (CFU mL⁻¹) for all microorganisms. A microdilution assay was performed at 96-microplate using blank and AgNPs starting at 1:4 dilution. In order to evaluate the antibacterial properties, growth inhibition was measured by turbidimetry after 24 h of incubation at 37 °C. The minimum inhibitory concentration (MIC), which is defined as the lowest concentration of antimicrobial agent that is able to inhibit bacterial growth after overnight incubation, was determined. All antimicrobial parameters were studied in triplicate.

Cytotoxicity assay

The toxicity of blank and AgNPs samples was evaluated using the Baby Hamster Kidney (BHK) cell line through the MTT assay according to Mosmann.³⁵ Briefly, 10^4 cells were cultured in standard conditions (DMEM containing 10% fetal calf serum and 1% penicillin/streptomycin at 37 °C and 5% CO₂) for 24 h in 96-well plates. Then cells were incubated with blank or AgNPs at 1:2 to 1:64 serial dilution for another 24 h. MTT [3-(4,5-dimethylthiazol-2-yl)-2,5-diphenyltetrazolium bromide] solution (0.5 mg mL⁻¹) was added to cells in serum-free medium and incubated for 4 h at 37 °C. Formazan crystals were dissolved with DMSO and the plate was read at 570 nm using Anthos200RT Spectrophotometer (Anthos, Germany). Negative control (100% viability) consisted of untreated cells and positive control (0% viability) were cells treated with 2% Triton X-100 (Sigma, USA).

Results and discussion

Ionic silsesquioxane

In this work, the ionic silsesquioxane containing the 1,4-diazoniabicyclo[2.2.2]octane nitrate group, SiDb(NO₃)₂, was synthesized. It is important to emphasize that it is the first report

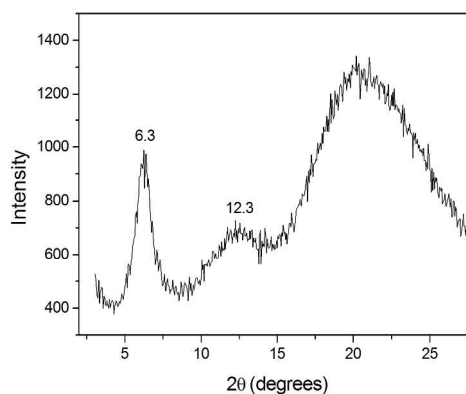


Fig 2. X-ray diffractogram for SiDb(NO₃)₂

of the preparation of the ionic silsesquioxane SiDb(NO₃)₂ and its use to promote the silver nanoparticles stabilization.

The X-ray diffraction result for SiDb(NO₃)₂ (Figure 2) revealed the presence of three peaks, 2θ near 6.3°, 12.3° and 20°. This result is in accordance with previous report for the SiDb(Cl)₂ silsesquioxane, where chloride was the counter ion.³⁶ The large peak, with 2θ near 20° is characteristic of amorphous silica.³³ The peaks with angle 2θ of 6.3° and 12.3° corresponding to Bragg distances of 1.40 nm and 0.72 nm, respectively, indicate the existence of organized structure.^{33,36}

The ¹³C and ²⁹Si-NMR spectra of the SiDb(NO₃)₂ in solid state are presented in Figure 3. In the ¹³C-NMR spectrum (Figure 3A), the signals at 9.95, 16.0, and 66.5 ppm correspond to the *n*-propyl group. The signal at 51.6 ppm is related to the carbon of the DABCO group and the signal at 44.9 ppm is due to the remaining methoxy groups.^{34,36} In the ²⁹Si-NMR spectrum (Figure 3B) it was observed only T species,^{36,37} since the silsesquioxane was gellified in the absence of tetraalkylorthosilicate. The signals at -59.1 and -68.5 ppm were ascribed to T² [C-Si⁺(OR)(OSi)₂] and T³ [C-Si⁺(OSi)₃] silicon species, indicating a high grade of crosslinking.^{36,37} These results were similar to the previous reports for SiDb(Cl)₂,^{34,36} indicating that the ion-exchange process did not affect the silsesquioxane structure.^{36,37}

Silver nanoparticles/ionic silsesquioxane system

The ionic silsesquioxane showed to be soluble in water due to the presence of charged groups, which allowed stabilizing silver nanoparticles (AgNPs) in aqueous medium. This property proves to be especially important for biological and medical applications because all of these fields comprise aqueous media. The obtained colloidal dispersion stabilized by ionic silsesquioxane showed yellow color, typical of spherical and well-dispersed silver nanoparticles,²⁰ and their optical absorption spectra, freshly prepared and 12 month later, are presented in Figure 4. The spectrum shows a band with maximum at 410 nm due to the surface plasmon resonance, by the excitation of free electrons within the conduction band, leading to an in-phase oscillation.^{3,6} According to Mie's theory, only a single surface plasmon resonance band is expected in absorption spectra of spherical nanoparticles. On the other hand, anisotropic particles could give rise to two or more bands depending on the shape of the particles.

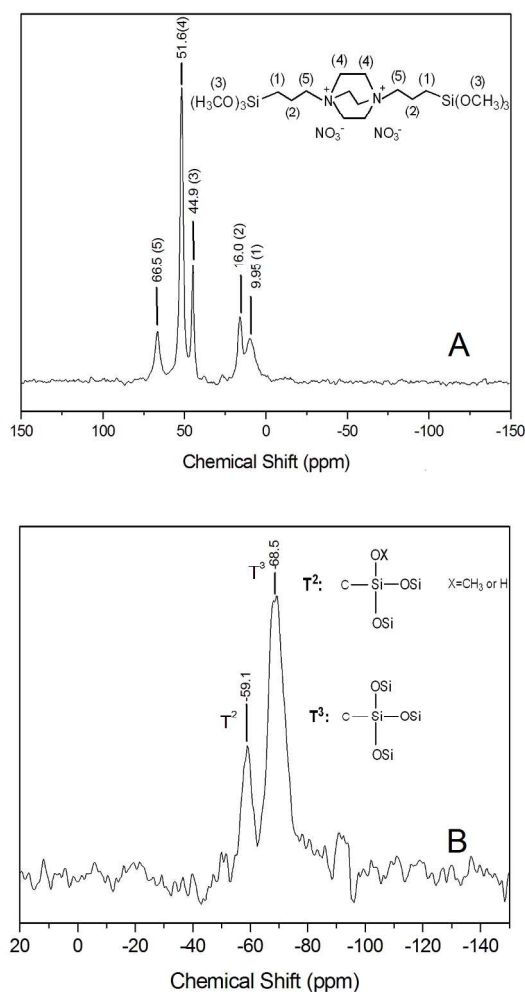


Fig 3. CP-MAS NMR spectra of $\text{SiDb}(\text{NO}_3)_2$ (A) ^{13}C and (B) ^{29}Si

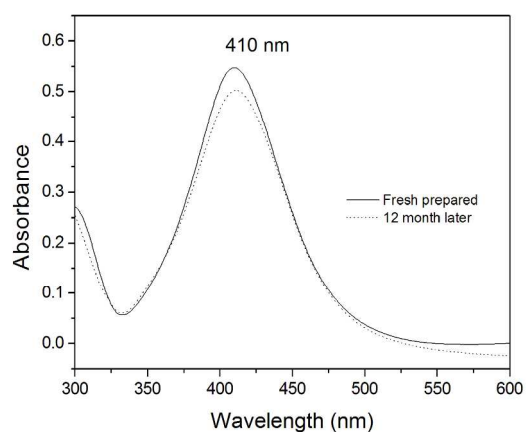


Fig 4. UV-Vis absorption spectra of AgNPs aqueous dispersion

Thus, spherical nanoparticles, disks, and triangular nanoplates of silver show one, two, and more peaks, respectively.¹⁸

A fraction obtained from a typical TEM image of AgNPs dispersion is presented in Figure 5. It is possible to observe that the nanoparticles have regular spherical shape. The nanoparticles size distribution histogram is also showed in the Figure 5. The obtained average diameter (d) was calculated from the original image containing 933 nanoparticles. The average diameter (d) was 4.9 nm, with a standard deviation (σ) of 2.6 nm. This value is in agreement with the UV-Vis absorption showed in Figure 4. It is important to point out that, the AgNPs aqueous dispersion is very stable, since no changes in the UV-Vis absorption maximum or in the average particle size could be detected after, at least, twelve months of storage (Figure 4). The dried silver nanoparticles/silsesquioxane system was submitted to XPS analysis. The Ag $3d_{5/2}$ and $3d_{3/2}$ occurred at binding energies of 373.9 and 367.6 eV, respectively, which correspond to metallic silver.^{38,39} However the presence of silver ions cannot be discarded, since the XPS peaks are very weak to allow estimate them.

In this work, ζ -potential analyses were performed for AgNPs aqueous dispersion and also for a reference sample, designated as blank, which is a similar aqueous solution containing all components of the AgNPs dispersion, except the silver nanoparticles. Although the ζ -potential was carried out in the pH range from 2 to 12, here are presented only the results for pH 7.5, which is near to the physiological pH. Both samples exhibit positive ζ -potential values, being +8.13, with standard deviation of 0.95, for blank sample and +24.7, with standard deviation of 2.3, for AgNPs dispersion.

Zeta (ζ)-potential is often used as an index of the magnitude of electrostatic interaction between colloidal particles and is thus a measure of colloidal stability of the dispersion.⁴⁰ It was reported that particles with ζ -potential above 25 mV (positive or negative) are considered to present highly charged surfaces and only above 40 mV (positive or negative) they are considered just to be stabilized by electrostatic effects.^{41,42} As already presented, our system is very stable even having showed +24.7 mV ζ -potential. The signal of the measured ζ -potential of AgNPs indicates that the particles have positive charge on their surface, therefore they are able to minimize their aggregation due to electrostatic repulsion.⁴³ However the stability of our system cannot be explained only considering electrostatic mechanism. The stabilization should present also a steric component, since the stabilizer is a polymer, a silica based hybrid material, which contain Si-O-Si linkages, as represented in the scheme of Figure 1. The positive ζ -potential of the blank sample was assigned to the presence of quaternary ammonium groups of the silsesquioxane.

Antibacterial tests

The *in vitro* antibacterial tests were performed against two Gram-negative (*E. coli* and *P. aeruginosa*) and one Gram-positive (*S. aureus*) bacteria. The start dispersion, before the dilutions, was $11.3 \times 10^{-6} \text{ mol mL}^{-1}$ of divalent 1,4-diazoniabicyclo[2.2.2]octane nitrate group used as stabilizer and $10.1 \times 10^{-6} \text{ g mL}^{-1}$ of silver. Table 1 shows the results of the antibacterial activity of blank and AgNPs samples.

It is possible to observe that both samples present a high activity in preventing the growth of bacteria, even at very low

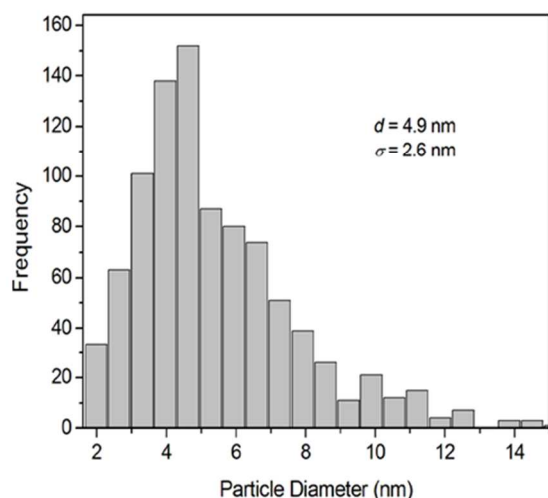


Fig.5. TEM image and AgNps size distribution

concentrations. The results show that at 1:4 dilution of blank and AgNPs samples inhibited bacterial growth for the three types of bacteria studied. However, at 1:8 dilution only sample containing AgNPs inhibited the growth of *S. aureus* and *E. coli*. On the other hand, *P. aeruginosa* growth was not inhibited by AgNPs at 1:8 dilution, whereas *S. aureus* growth was inhibited by AgNPs even at 1:16 dilution.

Considering the inhibition susceptibility of the bacteria, it was observed in the present work that *S. aureus* (Gram-positive) is comparatively more sensitive to the AgNPs dispersion than *E. coli* and *P. aeruginosa*, both Gram-negative (Table 1). These results are in agreement with those reported by other,⁴⁴ and can be explained by the differences in the cell wall structure of the strains. The outer membrane may act as a barrier, preventing the action of the bactericide agent on cytoplasmic membrane.⁴⁵ Gram-negative bacteria are characterized by cell walls which consist of two membranes: an inner membrane based on to the action of antibiotics.³³ Similarly, the quaternary ammonium groups tend to adhere to the cytoplasmic membrane of the bacteria by electrostatic interaction.³¹ Thus, the presence of

quaternary groups in the ionic silsesquioxane structure justifies the appreciable antibacterial activity even in the absence of silver nanoparticles (blank sample).

In the presence of AgNPs the antibacterial activity was significantly enhanced, due to the joint action of nanoparticles and the presumable silver ions contained in the dispersion.^{14,46,47} As it was already discussed, the AgNPs present positive ζ -potential, indicating positive surface charge, while the bacterial cells are negatively charged and show negative ζ -potential, over a wide pH range.⁴⁴ Thus, the AgNPs improve the electrostatic interaction with the bacterial cell surface, according to previous reports.^{45,48} Therefore, the synergistic effect of silver ions and nanoparticles with quaternary ammonium group of silsesquioxane leads to an antimicrobial activity much more efficient.

The performance of AgNPs stabilized by $\text{SiDb}(\text{NO}_3)_2$ against the *S. aureus*, *E. coli* or *P. aeruginosa* presented in this work was compared to different silver nanoparticle systems already reported, in similar conditions, and a detailed comparison is showed in Table 2. It can be observed that two previous reports showed lower MIC values, against *E. coli* or *P. aeruginosa* Gram-negative bacteria, than our results (Table 2). However, the performance, of AgNPs stabilized by $\text{SiDb}(\text{NO}_3)_2$ was superior to most of the other cited systems (Table 2). Regarding the *S. aureus* Gram-positive bacterium, the AgNPs stabilized by $\text{SiDb}(\text{NO}_3)_2$ was the best one. Therefore, this AgNPs is a new and promising system to be applied as antibacterial agent.

Cytotoxicity assay

The AgNPs system developed in this work is expected to be used in the health field, water treatment and food packaging coating, wherein the cytotoxicity grade is an important indicator for usage safety. For this purpose, it was used the MTT reduction tests assuming that an inhibition of cell growth less than 30%, when compared to negative controls, indicates biocompatibility and free of cytotoxicity.^{49,50} The cytotoxicity of AgNPs dispersion results are shown in Table 3.

As shown in Table 3, samples containing AgNPs show higher toxicity than samples without AgNPs (blank) in BHK cells. For samples containing AgNPs 1:4 dilution, it was observed a higher toxicity, while for superior dilutions, a cell viability was above 70%. Since AgNPs are effective against bacterial growth at dilutions of 1:8 or 1:16 (Table 3), the cytotoxicity assay shows that these nanoparticles are relatively safe for mammalian cells at the desired concentrations.

In general, the cytotoxicity is related to the zeta potential value, the higher zeta potential the higher cytotoxicity.⁴⁸ Although the zeta potential of our AgNPs dispersion was +24.7 mV, it presented low cytotoxicity. It was already reported that system with similar zeta potential showed also low cytotoxicity.^{48,51,52} Therefore, the high stability presented by our AgNPs dispersion (Figure 2) and the zeta potential value indicate that particles stabilization have electrostatic and also steric contributions, as discussed in previous section. Possibly the interaction between positive charges of our polymeric system with the BHK cell wall can be hindered by the steric structure of silsesquioxane that presents Si-O-Si linkages.

5 **Table 1** Antibacterial activity of blank (A) and AgNPs (B) samples.

	Dilution					
	1:4		1:8		1:16	
	A	B	A	B	A	B
[SiDb(NO ₃) ₂] (10 ⁻⁶ mol mL ⁻¹)	2.3	2.3	1.3	1.3	0.7	0.7
[Ag] (10 ⁻⁶ g mL ⁻¹)		2.0		1.1		0.6
Bacteria						
<i>S. aureus</i>	-	-	+	-	+	-
<i>E. coli</i>	-	-	+	-	+	+
<i>P. aeruginosa</i>	-	-	+	+	+	+

+ = bacterial growth; - = absence of bacterial growth; A = blank; B = AgNPs

Table 2 Comparative performance of silver nanoparticles against *S. aureus*, *E. coli* and *P. aeruginosa*.

AgNPs / stabilizer system	Nanoparticles average size (nm)	Bacterial species	Bacterial cell concentration (CFU mL ⁻¹)	MIC (10 ⁻⁶ g mL ⁻¹)	Reference
AgNPs / chitosan	6-8	<i>S. aureus</i> <i>E. coli</i>	10 ⁵	10.0 10.0	(20)
AgNPs / Na ⁺ -poly (γ-glutamic acid)	17-37	<i>S. aureus</i> <i>P. aeruginosa</i>	10 ⁵	1.2 2.1	(49)
AgNPs / Na ⁺ dodecyl sulfate	24	<i>S. aureus</i> <i>E. coli</i> <i>P. aeruginosa</i>	10 ⁵ - 10 ⁶	259 259 6.58	(53)
AgNPs / Na ⁺ dodecyl sulfate	9	<i>S. aureus</i> <i>E. coli</i> <i>P. aeruginosa</i>	10 ⁵ - 10 ⁶	14.38 14.38 14.38	(53)
Ag / Na ⁺ -gallic acid	20-25	<i>S. aureus</i> <i>E. coli</i> <i>P. aeruginosa</i>	-	0.74 0.53 0.37	(54)
Ag / Na ⁺ -gallic acid	7	<i>S. aureus</i> <i>E. coli</i>	10 ⁵	7.5 6.25	(55)
Ag / Na ⁺ -gallic acid	29	<i>S. aureus</i> <i>E. coli</i>	10 ⁵	16.67 13.02	(55)
Ag / Na ⁺ -gallic acid	89	<i>S. aureus</i> <i>E. coli</i>	10 ⁵	33.71 11.79	(55)
AgNPs / cystein	14.5	<i>S. aureus</i> <i>E. coli</i> <i>P. aeruginosa</i>	5×10 ⁸	9.72 4.32 6.48	(56)
AgNPs / β-cyclodextrin	4-7	<i>S. aureus</i> <i>E. coli</i> <i>P. aeruginosa</i>	10 ⁶	3.12 3.12 12.5	(57)
AgNPs / PVO-b-PAN copolymer	4-28	<i>S. aureus</i> <i>E. coli</i> <i>P. aeruginosa</i>	10 ⁸	2.88 0.36 0.36	(58)
AgNPs / SiDb(NO ₃) ₂	4.9	<i>S. aureus</i> <i>E. coli</i> <i>P. aeruginosa</i>	10 ⁸	0.60 1.12 2.03	This work

Cite this: DOI: 10.1039/c0xx00000x

ARTICLE TYPE

www.rsc.org/xxxxxx

Table 3 MTT results for the blank and AgNPs.

Sample	Dilution	[SiDb(NO ₃) ₂] (10 ⁻⁶ mol mL ⁻¹)	[Ag] (10 ⁻⁶ g mL ⁻¹)	Relative (%) growth rate
Blank	1:4	2.3	-	88 ± 6
	1:8	1.3	-	100 ± 8
	1:16	0.7	-	90 ± 5
AgNPs	1:4	2.3	2.0	58 ± 6
	1:8	1.3	1.1	90 ± 4
	1:16	0.7	0.6	78 ± 5

Conclusions

The ionic silsesquioxane SiDb(NO₃)₂ containing the quaternary ammonium group, the 1,4-diazoniabicyclo[2.2.2]octane and nitrate as counter ion was obtained. It was successfully applied for the first time to the synthesis of silver nanoparticles in aqueous medium, resulting in the formation of spherical nanoparticles with a predominant size distribution below 10 nm and average diameter of 4.9 nm. The AgNPs stabilized by SiDb(NO₃)₂ aqueous dispersion showed high antibacterial activity against *E. coli*, *P. aeruginosa* and *S. aureus* bacteria, when compared to the other systems. The AgNPs stabilized by SiDb(NO₃)₂ show interesting features, since they present charge that allow their water solubility, contributing to the stabilization and antibacterial activity. Additionally, they also present silica moiety that improves the metal nanoparticle stabilization reducing their cytotoxicity.

Acknowledgement

The authors are grateful to CNPQ (Conselho Nacional de Desenvolvimento Científico e Tecnológico), FAPERGS (Fundação de Amparo à Pesquisa do Estado do Rio Grande do Sul) and CAPES (Coordenação de Aperfeiçoamento Pessoal de Nível Superior) for their financial support and fellowships. We also thank the Centro de Microscopia Eletrônica da Universidade Federal do Rio Grande do Sul for TEM images. We thank the Professor Richard Landers and Rita Vinhas of Unicamp for XPS analysis.

Notes and references

^a Instituto de Química, Universidade Federal do Rio Grande do Sul (UFRGS), CP 15003, CEP 91501-970, Porto Alegre, RS, Brazil.

^b Hospital de Clínicas de Porto Alegre, Rua Ramiro Barcelos, 2350, CEP 90035-903, Porto Alegre, RS, Brazil.

† Electronic Supplementary Information (ESI) available: [details of any supplementary information available should be included here]. See DOI: 10.1039/b000000x/

- O. A. Belyakova and Y. L. Slovokhotov, *Russ. Chem. Bull.* 2003, **52**, 2299-2327.
- M. -C. Daniel and D. Astruc, *Chem. Rev.*, 2004, **104**, 293-346.
- A. Akjouj, G. Lévêque, S. Szunerits, Y. Pennec, B. Djafari-Rouhani, R. Boukherroub and L. Dobrzynski, *Surface Sci. Reports*, 2013, **68**, 1-67.
- S. Liu and Z. Tang, *J. Mater. Chem.*, 2010, **20**, 24-35.
- K. K. Y. Wong and X. L. Liu, *Pediatr. Surg. Int.* 2012, **28**, 943-951.
- S. Eustis and M. A. El-Sayed, *Chem. Soc. Rev.*, 2006, **35**, 209-217.
- J. N. Anker, W. P. Hall, O. Lyandres, N. C. Shah, J. Zhao and R. P. V. Duyne, *Nature Mater.*, 2008, **7**, 442-453.
- J. Dupont, *Acc. Chem. Res.* 2011, **44**, 1223-1231.
- R. Taylor, S. Coulombe, T. Otanicar, P. Phelan, A. Gunawan, W. Lv, G. Rosengarten, R. Prasher and H. Tyagi, *J. Appl. Phys.* 2013, **113**, 011301-19.
- S. Nath, S. Jana, M. Pradhan and T. Pal, *J. Colloid Interface Sci.*, 2010, **341**, 333-352.
- T. -H. Tran and T. -D. Nguyen, *Colloids Surfaces B*, 2011, **88**, 1-22.
- P. Saint-Cricq, J. Wang, A. Sugawara-Narutaki, A. Shimajima and Tatsuya Okubo, *J. Mater. Chem. B*, 2013, **1**, 2451-2454.
- K. Chaloupka, Y. Malam and A. M. Seifalian, *Trends Biotechnol.* 2010, **28**, 580-588.
- C. Marambio-Jones and E. M. V. Hoek, *J. Nanopart. Res.* 2010, **12**, 1531-1551.
- H. H. Park, S. J. Park, G. P. Kob and K. Woo, *J. Mater. Chem. B*, 2013, **1**, 2701-2709.
- J. R. Morones, J. L. Elechiguerra, A. Camacho, K. Holt, J. B. Kouri, J. T. Ramirez and M. J. Yacaman, *Nanotechnol.* 2005, **16**, 2346-2356.
- P. Lackner, R. Beer, G. Broessner, R. Helbok, K. Galiano, C. Pleifer, B. Pfausler, C. Brenneis, C. Huck, K. Engelhardt, A. A. Obwegeser and E. Schmutzhard, *Neurocrit. Care* 2008, **8**, 360-365.
- S. Pal, Y. K. Tak and J. M. Song, *Appl. Environ. Microbiol.* 2007, **73**, 1712-1720.
- J. S. Kim, E. Kuk, K. N. Yu, J. -H. Kim, S. J. Park, H. J. Lee, S. H. Kim, Y. H. Park, C. -Y. Hwang, Y. -K. Kim, Y. -S. Lee, D. H. Jeong and M. -H. Cho, *Nanomedicine*, 2007, **3**, 95-101.
- D. Wei, W. Sun, W. Qian, Y. Ye and X. Ma, *Carbohydr. Res.*, 2009, **344**, 2375-2382.
- A. Panáček, L. Kvítek, R. Prucek, M. Kolár, R. Vecerová, N. Pizúrová, V. K. Sharma, T. Nevečná and R. Zboril, *J. Phys. Chem. B*, 2006, **110**, 16248-16253.
- M. R. Nunes, Y. Gushikem, R. Landers, J. Dupont, T. M. H. Costa and E. V. Benvenutti, *J. Sol-Gel Sci. Technol.* 2012, **63**, 258-265.
- E. W. de Menezes, M. R. Nunes, L. T. Arenas, S. L. P. Dias, I. T. S. Garcia, Y. Gushikem, T. M. H. Costa and E. V. Benvenutti, *J. Solid State Electrochem.*, 2012, **16**, 3703-3713.
- Y. Gushikem, E. V. Benvenutti and Y. V. Kholin, *Pure Appl. Chem.*, 2008, **80**, 1593-1611.
- L. T. Arenas, A. Langaro, Y. Gushikem, C. C. Moro, E. V. Benvenutti and T. M. H. Costa, *J. Sol-Gel Sci. Technol.*, 2003, **28**, 51-56.
- L. D. Melo, E. M. Mamizuka and A. M. Carmona-Ribeiro, *Langmuir*, 2010, **26**, 12300-12306.
- D. Demberelnyamba, K. -S. Kim, S. Choi, S. -Y. Park, H. Lee, C. -J. Kim and I. -D. Yoo, *Bioorg. Med. Chem.*, 2004, **12**, 853-857.
- B. Rasines, J. M. Hernández-Ros, N. de las Cuevas, J. L. Copa-Patiño, J. Soliveri, M. A. Muñoz-Fernández, R. Gómez and F. J. de la Mata, *Dalton Trans.*, 2009, 8704-8713.

29. K. Rózga-Wijas, U. Mizerska, W. Fortuniak, J. Chojnowski, R. Hałasa and W. Werel, *J. Inorg. Organomet. Polym.*, 2007, **17**, 605-613.
30. R. R. Pant, J. L. Buckley, P. A. Fulmer, J. H. Wynne, D. M. McCluskey and J. P. Phillips, *J. App. Polymer Sci.*, 2008, **110**, 3080-3086.
31. J. Huang, R. R. Koepsel, H. Murata, W. Wu, S. B. Lee, T. Kowalewski, A. J. Russell and K. Matyjaszewski, *Langmuir*, 2008, **24**, 6785-6795.
- 10 32. K. Lewis and A. M. Klibanov, *Trends Biotechnol.*, 2005, **23**, 343-348.
33. B. Simionescu, I. -E. Bordianu, M. Aflori, F. Doroftei, M. Mares, X. Patras, A. Nicolescu and M. Olaru, *Mater. Chem. Phys.* 2012, **134**, 190-199.
- 15 34. L. T. Arenas, S. L. P. Dias, C. C. Moro, T. M. H. Costa, E. V. Benvenuti, A. M. S. Lucho and Y. Gushikem, *J. Colloid Interface Sci.* 2006, **297**, 244-250.
35. T. Mosmann, *J. Immunol. Methods*, 1983, **65**, 55-63.
36. L. T. Arenas, A. C. Pinheiro, J. D. Ferreira, P. R. Livotto, V. P. Pereira, M. R. Gallas, Y. Gushikem, T. M. H. Costa and E. V. Benvenuti, *J. Colloid Interface Sci.*, 2008, **318**, 96-102.
- 20 37. E. W. de Menezes, E. C. Lima, B. Royer, F. E. de Souza, B. D. dos Santos, J. R. Gregório, T. M. H. Costa, Y. Gushikem and E. V. Benvenuti, *J. Colloid Interface Sci.*, 2012, **378**, 10-20.
- 25 38. L. Zhang, Y. H. Shen, A. J. Xie, S. K. Li and Y. M. Li, *J. Mater. Chem.*, 2009, **19**, 1884-1893
39. W. Wang, Y. Jiang, Y. Liao, M. Tian, H. Zou, L. Zhang, *J. Colloid Interface Sci.* 2011, **358**, 567-574.
40. B. White, S. Banerjee, S. O'Brien, N. J. Turro and I. P. Herman, *J. Phys. Chem. C*, 2007, **111**, 13684-13690.
- 30 41. W. Yu and H. Xie, *J. Nanomater.*, 2012, **2012**, 435873-435890.
42. S. Tanvir, F. Oudet, S. Pulvina and W. A. Anderson, *Enzyme Microb. Technol.*, 2012, **51**, 231-236.
43. I. Medina-Ramírez, M. González-García and J. L. Liu, *J. Mater. Sci.*, 2009, **44**, 6325-6332.
- 35 44. S. S. Khan, A. Mukherjee and N. Chandrasekaran, *Colloids Surfaces B*, 2011, **87**, 129-138.
45. R. S. Patil, M. R. Kokate, P. P. Salvi and S. S. Kolekar, *C. R. Chimie*, 2011, **14**, 1122-1127.
46. J. R. Morones, J. L. Elechiguerra, A. Camacho, K. Holt, J. B. Kouri, J. T. Ram and M. J. Yacaman, *Nanotech* 2005, **16**, 2346-2353.
47. H. Y. Lee, H. K. Park, Y. M. Lee, K. Kim and S. B. Park, *Chem. Comm.* 2007, 2959-2961.
48. A. E. Nel, L. Mädler, D. Velegol, T. Xia, E. M. V. Hoek, P. Somasundaran, F. Klaessig, V. Castranova and M. Thompson, *Nature Mater.* 2009, **8**, 543-557.
- 45 49. D. -G. Yu, *Colloids Surfaces B*, 2007, **59**, 171-178.
50. E. Borenfreund and O Borrero, *Cell Biol. Toxicol.* 1984, **1**, 55-65.
51. Y. Ding, X. Bian, W. Yao, R. Li, D. Ding, Y. Hu, X. Jiang,; Y. Hu, *Appl. Mat. Interf.* 2010, **2**, 1456-1465.
- 50 52. W. Lesniak, A. U. Bielinska, K. Sun, K. W. Janczak, X. Shi, J. R. Baker and L. P. Balogh, *Nano Letters*. 2005, **5**, 2123-2130.
53. M. Guzman, J. Dille and S. Godet, *Nanomedicine*, 2012, **8**, 37-45.
54. F. Martinez-Gutierrez, P. L. Olive, A. Banuelos, E. Orrantia, N. Nino, E. M. Sanchez, F. Ruiz, H. Bach and Y. Av-Gay, *Nanomedicine*, 2010, **6**, 681-688.
- 55 55. G. A. Martínez-Castañón, N. Niño-Martínez, F. Martínez-Gutierrez, J. R. Martínez-Mendoza and F. Ruiz, *J. Nanopart. Res.*, 2008, **10**, 1343-1348.
- 60 56. M. Roy, P. Mukherjee, B. P. Mandal, R. K. Sharma, A. K. Tyagi and S. P. Kale, *RSC Adv.*, 2012, **2**, 6496-6503.
57. S. Jaiswal, B. Duffy, A. K. Jaiswal, N. Stobie and P. McHale, *Int. J. Antimicrob. Agents*, 2010, **36**, 280-283 (2010).
58. R. Bryaskova, D. Pencheva, M. Kyulavska, D. Bozukova, A. Debuigne and C. Detrembleur, *J. Colloid Interface Sci.*, 2010, **344**, 424-428.
- 65